Assessing powder flowability at low stresses using ball indentation method: Evaluation of constraint factor

U. Zafar [1], C. Hare [2], A. Hassanpour, M. Ghadiri *

School of Chemical and Process Engineering, University of Leeds, Leeds LS2 9JT, UK

ABSTRACT

Powders can exhibit different flow behaviour resulting from a combination of physical properties of the material and equipment design. Problems with powder flow are ubiquitous in process industry and become prominent when dealing with fine and cohesive powders. It is therefore of great importance to characterise the flowability of cohesive materials for better process control. Powder flowability is commonly assessed under relatively high preconsolidation loads using shear cell and uniaxial compression methods by which the unconfined yield strength (Y) is evaluated as a function of the applied load. However, these techniques are typically limited to applied stresses greater than 1 kPa and require a relatively large quantity of powder. To overcome these limitations, the recently developed Ball Indentation Method (BIM) is used in this work for assessing powder flow behaviour at low stress levels. The unconfined yield strength (Y) is inferred from the resistance to ball penetration into the surface of a powder bed, based on the method for measurement of hardness (H). This requires the flow resistance, represented by hardness, to be related to the unconfined yield strength by a proportionality factor termed the constraint factor, C, following the analogy with yield stress measurement in continuum solids, i.e. $Y=H/C$. The constraint factor for silanised glass ballotini, calcium carbonate, α-lactose monohydrate, Avicel and limestone is evaluated and reported here. It is shown that the unconfined yield strength inferred by this method correlates well with those from the uniaxial compression and shear cell measurement. The characterisation of the constraint factor makes it possible to use BIM for powder flowability testing at low stress levels and using a very small powder quantity. This is highly desirable for applications such as capsule filling, tableting and dry powder inhaler devices.

© 2021 The Authors. Published by Elsevier B.V. This is an open access article under the CC BY license (http://creativecommons.org/licenses/by/4.0/).

1. Introduction

The characterisation of bulk behaviour of cohesive powders is very important in processing of particulate solids, e.g. for reliable powder flow out of storage vessels. The bulk mechanical properties of cohesive powders have been analysed extensively for large operational scales and applied stresses, typical of those prevailing in storage vessels. However, for the pharmaceutical applications, such as filling and dosing of powders in capsules and for dispersion in dry powder inhalers, characterisation of small quantities of particles under very low applied loads is required.

There are various qualitative methods developed and frequently used for assessing powder flowability due to their simplicity. These

include angle of repose (AOR) [1], Carr Index [2], Hausner ratio [3], avalanche angle [4], funnel discharge [5], the Hosokawa powder tester PT-X (Hosokawa Micron B·V) and powder flow tester using a rotating drum, recently commercialised by Granutools, Awans, Belgium. However, parameters obtained from these tests cannot easily be related to macroscopic bulk properties governing flow behaviour, i.e. bulk cohesion. However, parameters obtained from these tests cannot easily be related to macroscopic bulk properties governing flow behaviour needed for bulk powder storage design procedures, i.e. bulk cohesion and friction as obtained from shear cell testing. Schulze [6] suggested some criteria that a test apparatus must have in order to provide quantitative results. Some of the more important requirements are the possibility of measuring the change in strength with time, providing a reproducible load application for compression, and the possibility for measuring low preconsolidation stresses. There are a number of techniques satisfying these criteria for assessing the flow behaviour of powders. These include the uniaxial test methods, e.g. Edinburgh Powder Tester, evaluated by Bell et al. [7] and recently manufactured commercially by Freeman Technology, Twekesbury, UK, Environmental Caking Rig [8] and shear cells, e.g. Jenike [9], Peschl shear cell, the Schulze

ring shear tester [6] and Brookfield powder tester [10]. For shear cell testers, the bulk cohesion and unconfined yield strength can only be measured reliably at applied loads typically larger than 1 kPa, and extension to lower stress levels are generally made by extrapolation. In some cases, the yield locus of a powder is described by the non-linear Warren-Spring model [11], but most often a straight line is fitted to the yield locus. However, these tests are generally not capable of handling measurements for applied loads much less than 1 kPa [12,13].

More recently-developed techniques for assessing the flow behaviour of powders focus on low stress ranges, such as the SSSpin Tester – which utilises a centrifugal force field to measure the unconfined yield strength [40], the Sevilla Powder Tester [14] and the Raining Bed Method [15] – which directly measure the tensile yield strength of the powder, the Ball Indentation Method [16] - which measures the flow resistance of a ball indenter deforming a powder bed, i.e. hardness, the FT4 powder rheometer of Freeman Technology [17] and also that of Anton Paar (Anton Paar GmbH, Graz, Austria), which measure the resistance to motion of a rotating impeller in a powder bed. The factors influencing the measurements of FT4 have recently been analysed by [18,19]. Also those related to the operation of Anton Paar rheometer have been analysed by [20]. Zafar et al. [21] compared the test results of the Sevilla Powder Tester, Raining Bed Method and Ball Indentation Method with those from the standard Schulze shear cell tester. A reasonably good correlation between all the methods was reported for some but not for all the methods. However, in the case of shear cell test method, extrapolation of the yield locus to lower loads was found unreliable. With the exception of Ball Indentation Method, the rest require relatively large quantities of powder. This is not possible in a number of instances, e.g. in industries such as nuclear and pharmaceuticals, due to safety constraints, cost of material and lack of availability at the early stages of development.

The indentation test has been tried and tested extensively for continuum solids [22–25], using different methods of testing based on the geometry of the indenter. During the process of local plastic deformation around the indenter, the volume of yield material is surrounded by an elastically deformed region and cannot easily flow. This leads to a situation in which the local flow resistance, as represented by hardness, is larger than the plastic yield stress. Their ratio is defined as the constraint factor [26].

$$C = \frac{H}{Y} \qquad (1)$$

where C is the constraint factor, H is the hardness of the material and Y is the yield stress. Studies by Hill et al. [27], Tabor [26], and Fischer-Cripps [28] considered the spherical indenter to be rigid and the indented material to be rigid-perfectly plastic, and proposed a constraint factor of 3 based on their analyses.

The Ball Indentation Method (BIM) has been analysed experimentally by Zafar et al. [29] and by numerical simulations based on the Discrete Element Method by Pasha et al. [30], where the operation windows for indenter size, load range, test specimen size, etc. have been defined. For particulate solids, Y is taken as the unconfined yield stress and the constraint factor, C, is expected to be dependent on the single particle properties, such as particle size and shape, roughness, adhesion and friction coefficient [30]. However, a quantitative evaluation of the dependence of C on these factors has not been carried out so far. In this study the Ball Indentation Method is used to measure powder bed hardness under different preconsolidation stresses for a wide range of materials. Adopting the procedure laid out by Zafar et al. [29], the Ball Indentation Method is analysed and the constraint factor for a number of materials with different properties is determined. For this purpose, the unconfined yield strength is measured using both the uniaxial compression test and ring shear tester. The outcome provides a better understanding of powder flow behaviour at low preconsolidation stresses.

Table 1
Test materials used in this work.

Powder	Material	Supplier
Glass ballotini	Sodium silicate	Omya
Durcal	Calcium carbonate	Omya
Avicel	Microcrystalline cellulose	BioChemika
Lactohale	α-lactose monohydrate	DFE Pharma
Limestone	Calcium carbonate (BCR)	Sigmaaldrich

Table 2
The characteristic sizes d_{10}, d_{50}, and d_{90} of the particle size distribution and the particle aspect ratio.

Material	d_{10} (μm)	d_{50} (μm)	d_{90} (μm)	Aspect ratio
Glass ballotini (45–63)	34.6	55.4	87.2	0.87
Glass ballotini (75–90)	60.2	83.2	115.6	–
Glass ballotini (90–125)	77.4	101.7	138.0	–
Durcal 15	1.8	14.7	30.3	0.69
Lactohale 230	2.5	10.0	22.9	0.70
Limestone	1.8	4.4	10.1	0.65
Avicel	17.8	41.8	89.5	0.64

2. Materials and methods

A number of powders with different physical and mechanical properties, morphologies and expected flow behaviours are selected, including silanised glass ballotini as a model test material for validating the DEM simulations. A hydrophobic silane (1, 7-Dichloro-1,1,3,3,5,5,7,7-octamethyltetrasiloxane) is used to make glass ballotini cohesive. The list of the test materials along with their suppliers are given in Table 1.

In this work, glass ballotini were sieved into different size cuts and the particle size distributions were measured using a Malvern Mastersizer 2000 (wet dispersion method) which is based on laser diffraction technique. The other test materials were obtained directly in narrow sieve cuts as supplied. For each material, the particle size distribution is averaged over several measurements. The particle shape is analysed using Malvern Morphologi G3 (Malvern Instruments, UK). The particles were dispersed on to a glass slide at 2 barg dispersion pressure with an injection time of 20 ms and settling time of 60 s using a sharp pulse of compressed air. The optical microscopy with a magnification lens of 50× was carried out, providing high quality information about particle morphology. The images of the scanned particles were saved for image analysis for determination of shape parameters, such aspect ratio (length/width). All recorded images were filtered to remove those for which an individual particle could not be identified. The characteristic sizes d_{10}, d_{50}, and d_{90} of the particle size distribution, obtained by wet dispersion method of the Malvern Mastersizer 2000, and the aspect ratio obtained by shape analysis using Malvern Morphologi G3 are given in Table 2.

The unconfined yield strength is an important representative of bulk powder cohesion, obtained by shear cell or uniaxial compression testing. It is the major principal stress of a free surface, which causes the bulk material to fail in the absence of the confining walls. Therefore, it is a good indicator of the powder flowability, when is expressed in terms of flow function coefficient (ffc), given by the ratio of major principal stress to unconfined yield strength. For the shear cell tests the Schulze Ring Shear (RST-XS) tester with the large cell (30 ml specimen volume) is used. The powder is pre-consolidated and pre-sheared and brought to a steady state at a given normal load in order to bring the sample to a known stress state, and then the shear force is measured at several applied normal loads below the pre-shear load, from which the bulk cohesion and unconfined yield strength are deduced. The powder is then sheared at a lower normal stress until incipient flow occurs. This procedure is repeated at different normal stresses to obtain further

points on the yield locus. The detailed procedure of the ring shear tester is described by Schwedes [3].

In the uniaxial compression test, the powder is compacted in a cylindrical die using an Instron 5566 mechanical testing machine (Instron Corp., USA) at a certain normal stress and then the walls of the die are removed, a force is then applied in the same direction as the preconsolidation force until the powder begins to flow. The force necessary to cause powder flow is measured from which the unconfined yield strength is calculated. The die has an inner diameter of 20 mm and is made of polytetrafluoroethylene (PTFE) in order to minimise wall friction. The direction of the major principal stress developed in this technique is not precisely known, but is expected to be inclined from the vertical due to the presence of wall friction, nevertheless, we take the assumption that the major principal stress is vertically aligned in this test and during ball indentation. Due to the absence of pre-shearing in the consolidation step of the uniaxial compression test, the packing state differs from that in a shear cell, and indeed contains a vertical variation in applied stress which is greatest close to the piston (top of the bed). For these reasons the uniaxial compression tests are not directly comparable to those of the shear cell. Nevertheless the wall friction of PTFE is small and the trends between the two techniques are quantitatively consistent [13,31,32].

In this work, the shear cell and uniaxial compression tests are used for comparison with the Ball Indentaion Method (BIM), using Eq. (1). The latter tests are carried out using the Instron 5566 mechanical testing machine (Instron Corp., USA). The same cylindrical die as of the unconfined yield strength measurements is used here. The loose powder is first directed into the die by sieving the powder into the die. In this method, the sample material is passed through a sieve with a mesh opening of approximately five times the mean particle diameter, which is directly placed above a funnel on top of the die. This procedure breaks cohesively-bonded clusters and agglomerates on sieving and packs them uniformly in the die [29]. The sample is then preconsolidated in the die by a stainless steel piston using a 10 N load cell, which has a resolution of 0.25 mN. The pre-consolidated samples are then subjected to indentation using a high precision spherical glass ball 2.38 mm diameter, supplied by Sigmund Lindner GmbH. The ball

is fixed to the end of a small rod using super glue which is mounted on the loading head of the machine. Ball indentation measurements are carried out following the standard operating procedure (SOP) set out by Zafar et al. [29], which ensures bed diameter and depth, indenter size and indentation depth are suitable to provide shear below the indentation zone and prevent wall effects.

3. Results

All experiments reported are carried out under ambient conditions, at a temperature range of 20-25 °C and relative humidity of 45–60%. The tests are done under quasi-static conditions for all three test methods, i.e. shear cell, uniaxial compression test and Ball Indentation Method.

3.1. Shear cell

Three repeats were carried out for each powder for each preconsolidation stress, to obtain yield loci under different pre-shear conditions. A family of yield loci is obtained for all the material samples and the unconfined yield strength as a function of major principal stress is plotted as shown in Fig. 1. The range of flow function coefficients for all the materials tested are shown in Table 3.

3.2. Uniaxial compression test

In the uniaxial compression test a minimum preconsolidation stress is required to avoid collapsing of the sample under gravity when the die walls are removed. This minimum stress is sometimes much higher than that acting in small process silos and hoppers. Furthermore, compaction of the powder sample under its own weight is neglected in the uniaxial compression test. Despite these limitations, this test method is commonly used for characterisation of powder flowability in terms of unconfined yield strength in industry due to its simplicity and short testing time.

The compression of bulk powders is dependent on the geometry of the bed, the friction between the powder bed and the containing walls
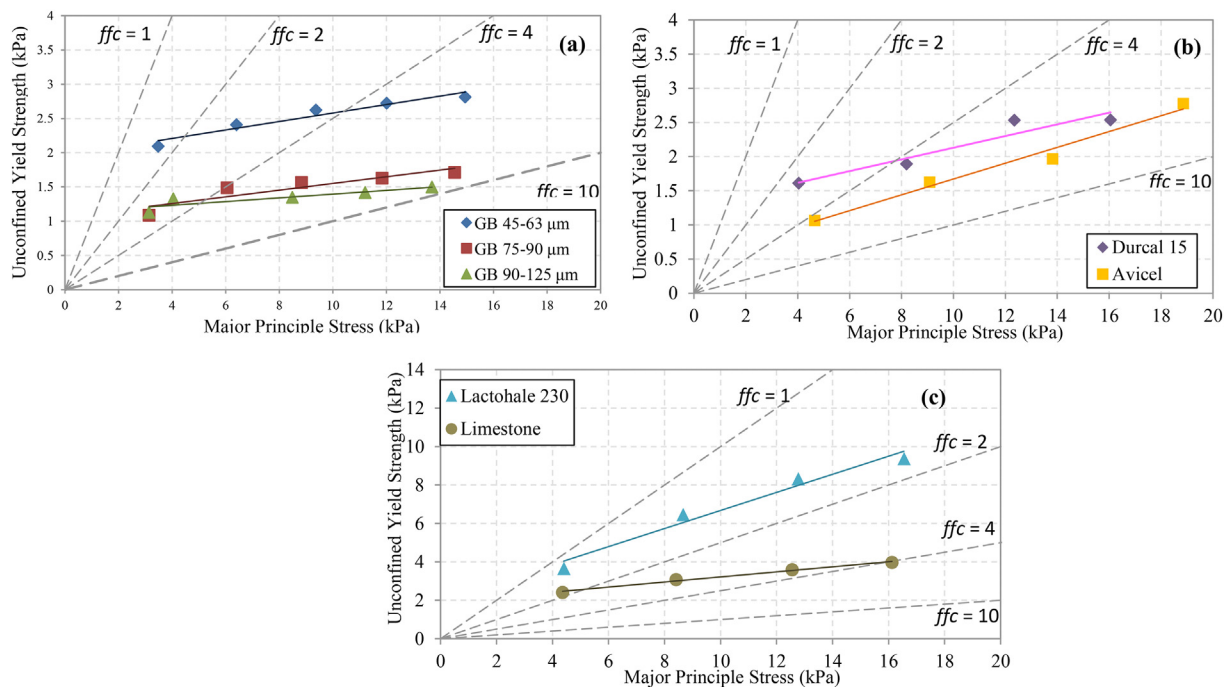

Fig. 1. Relationship between unconfined yield strength and major principal stress for (a): different sieve cuts of silanised glass beads; (b): Avicel and Durcal 15 and; (c): Lactohale 230 and limestone. Flowability regions: ffc > 10: free flowing; 4 < ffc < 10: easy flowing; 2 < ffc < 4: cohesive; ffc < 2: very cohesive.

Table 3
Flow function of test powders at normal stresses of 2–10 kPa.

Material	Flow function, ffc	Evaluation
Silanised glass beads 45–63 µm	1.7–5.3	Very cohesive - easy flowing
Silanised glass beads 75–90 µm	2.9–7.3	Cohesive - easy flowing
Silanised glass beads 90–125 µm	2.8–9.2	Cohesive - easy flowing
Avicel, d_{50} ~ 42 µm	4.4–7.5	Easy flowing
Durcal 15, d_{50} ~ 15 µm	2.5–7.2	Cohesive - easy flowing
Lactohale 230, d_{50} ~ 10 µm	1.34–2.6	Very cohesive
Limestone, d_{50} ~ 4 µm	1.8–4.9	Very cohesive – easy flowing

and piston, and the powder filling method [33,34]. There have been some efforts to overcome the die wall friction influence on the measurement using lubricants, as reviewed by [3,35]. Williams et al. [36] investigated the effect of height to diameter (L/D) ratio and showed that the unconfined yield strength decreased as L/D was increased until a critical value beyond which it became constant. This critical value occurs when the slip plane, initiated near to top platen, intersects the lower platen in the case of small L/D. In this case the failure in the specimen is constrained by the lower platen, due to friction, leading to a high stress required to initiate failure. This critical value is given by Eq. (2).

$$L/D = \tan(45° + \phi/2) \qquad (2)$$

where ϕ is the static angle of internal friction of the consolidated powder, which can be obtained from the yield locus generated from the shear cell results [3].

Uniaxial compression tests for several aspect ratios (L/D) were carried out on silanised glass beads at a preconsolidation stress of 10 kPa. After compression, the PTFE die is carefully lifted up. With wall friction being low, the compacted powder bed stays on the base and remains coherent, i.e. it does not collapse. It has very smooth side wall without any sign of damage from shear straining, implicitly indicating and that the surface is not noticeably disturbed by the friction between the container wall and powder bed (Fig. 2). The results obtained for different aspect ratios (L/D) are shown in Figs. 3.

The angle of internal friction for 90–125 µm silanised glass beads was measured by the shear cell tester at 10 kPa normal stress to be 23°, and the critical aspect ratio was therefore calculated to be 1.37. It is observed from Fig. 3 that if the aspect ratio is lower than the critical value then the applied pressure increases rapidly with initial displacement of the piston until a certain point after which the increase becomes gradual with no clear pressure peak, thus preventing measurement of the unconfined yield strength of the sample. When the aspect ratio is too small a barreling effect of the powder bed can be seen during the test. If the aspect ratio of the sample is close to at the critical value of L/D (L/D = 1.3), then the pressure increases with displacement and approaches an asymptotic value. However, above the critical value (e.g. L/D = 1.7, Fig. 3), the unconfined yield strength can be clearly observed as the bed fails.
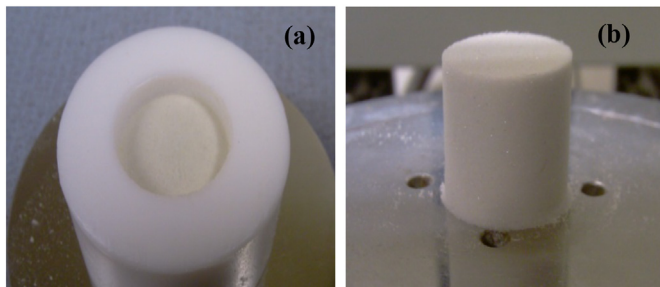

Fig. 2. Uniaxial compression test at 10 kPa; (a): compression of powder in the PTFE die; (b): compacted powder specimen after removal of die walls.
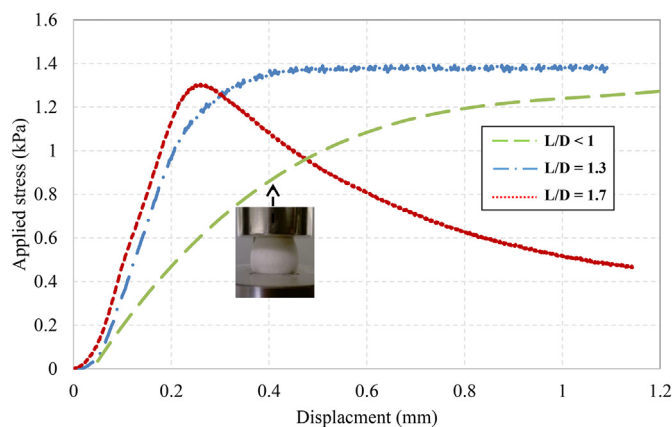

Fig. 3. Relationship between stress and displacement for an aspect ratio of less than 1, 1.3 and 1.7 for 90–125 µm silanised glass beads.

Table 4
Aspect ratio of all the test materials based on internal angle of friction as measured by Sculze shear cell tester.

Material	Internal angle of friction, °	Minimum L/D ratio
Silanised glass beads 45–63 µm	34	1.7
Silanised glass beads 75–90 µm	26	1.5
Silanised glass beads 90–125 µm	23	1.3
Avicel	44	2.3
Durcal 15	42	2.2
Lactohale 230	48	2.6
Limestone	43	2.3

The selection of aspect ratio (L/D) for the remaining tests is based on the internal angle of friction measurement obtained using the Schulze Ring Shear Tester at a preconsolidation stress of 10 kPa, the values given in Table 4. The results of the unconfined yield strength are shown in Fig. 4, with the error bars showing the span of three measurements. The test materials all show high resistance to flow, and thus have a large unconfined yield strength.

3.3. Ball indentation

Following the recommended procedure by Zafar et al. [29], the bed height of the compressed sample was at least 5 mm, i.e. kept greater than the minimum set out so that the indentation zone is not influenced by the base, but not large for the wall friction to affect the radial distribution of the pre-consolidation stress. Firstly, an investigation on the reliable indentation load range for hardness measurements was carried out for each test material. All the experimental results in this section are repeated three times under the same conditions and the error bars represent measurement span. The tests were carried out at a constant preconsolidation stress of 10 kPa in line with the unconfined yield strength measurements. Four indentation loads were applied in each case at separate positions made to determine the hardness. The results are shown in Fig. 5 for silanised glass beads. As expected, the hardness increases as the particle size is reduced, as the number of interparticle contacts per unit volume of packing increases accordingly. For the ball indentation experiment to be reliable, hardness must be independent of the indentation load in order to represent the bulk plastic yield stress. The hardness measurement remains roughly constant for all the three sieve cuts regardless of the indentation load as long as penetration depths does not exceed the indenter radius. A similar trend has been observed for all the other materials. Experiments were carried out to determine the hardness of the powder beds as a function of preconsolidation stress in the range 5–20 kPa. The results are shown
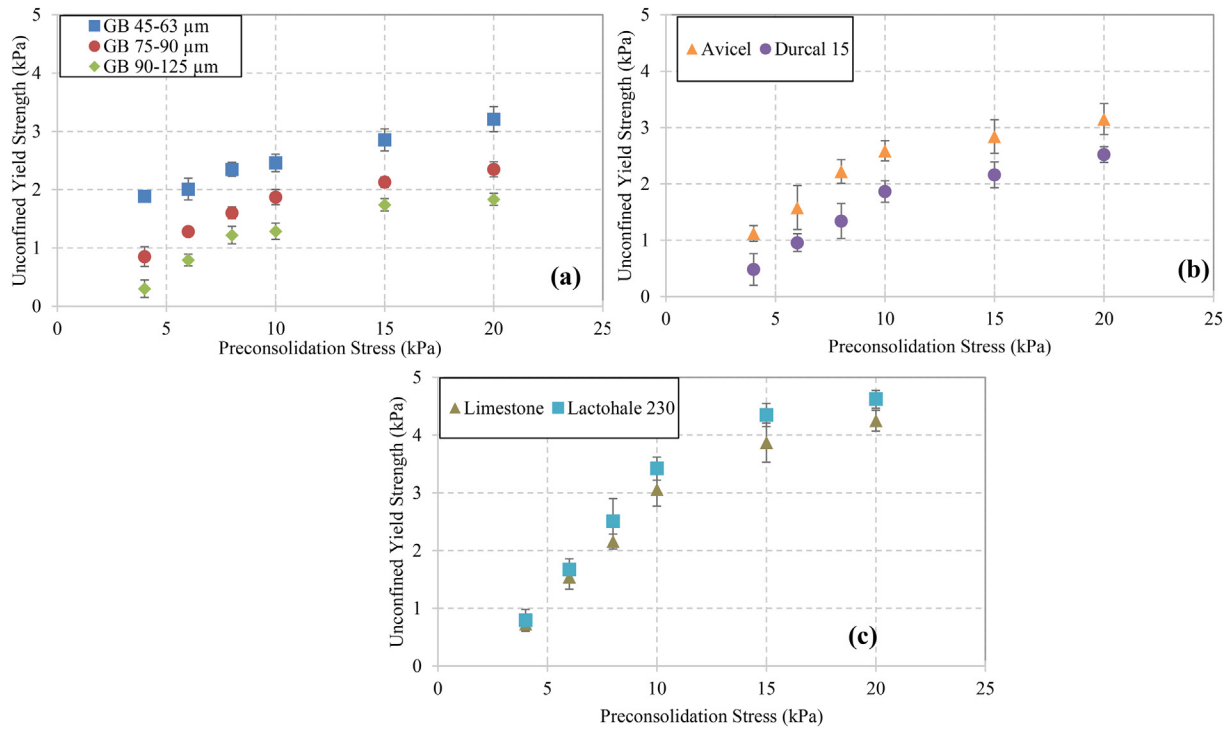
Fig. 4. Unconfined yield strength as a function of preconsolidation stress for (a): the sieve cuts of silanised glass beads; (b): Avicel and Durcal 15; (c): limestone and Lactohale 230.
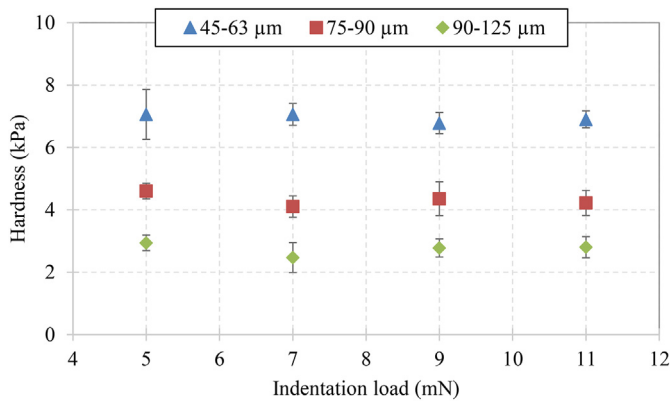

Fig. 5. Hardness measurement for different sieve cuts of silanised glass beads as a function of indentation load at 10 kPa preconsolidation stress.
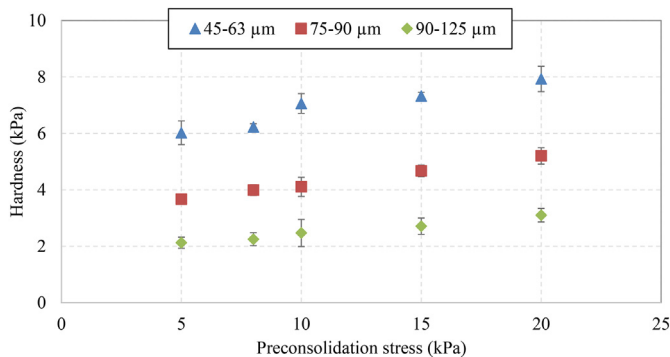

Fig. 7. Hardness as a function of preconsolidation stress for 45–63 μm silanised glass beads.

Fig. 6. Hardness as a function of preconsolidation stress for different sieve cuts of silanised glass beads at 7 mN indentation load.
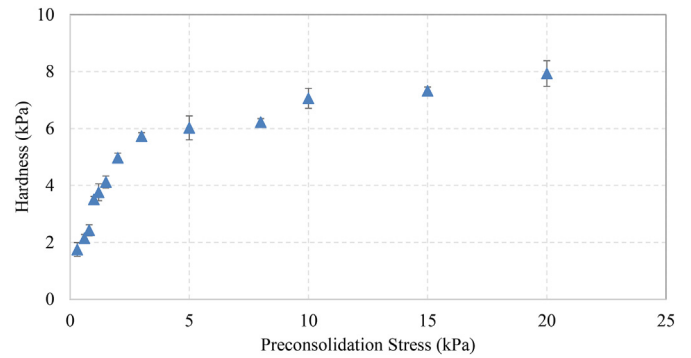
in Fig. 6, suggesting a roughly linear increase of the hardness as a function of the pre-consolidation load in this load range for all the sieve cuts of silanised glass beads. Interestingly, Stavrou et al. [37] have shown that there exists a clear correlation in the slopes of unconfined yield strength and packing fraction for the BIM test.

For ball indentation hardness measurements, it is important to have a powder bed which has a relatively flat surface. At high applied stresses above 5 kPa this is easily achieved by compression. However, at low preconsolidation stress levels this may be influenced by the filling technique. Using the sieved filling method, different samples were consolidated at low pressures below 1 kPa. Relatively smooth surfaces could be obtained for preconsolidation stresses of 200 Pa and above.

Ball indentation tests were also carried out at preconsolidation stresses lower than 5 kPa for 45–63 μm silanised glass beads. The results are combined with those at higher stresses and are shown in Fig. 7. Good repeatability is obtained even at low stress range. A similar trend has been observed for almost all the materials tested. Hardness measurements at low preconsolidation stresses (less than 5 kPa) for all the materials tested are shown in Fig. 8. It can be seen that Lactohale
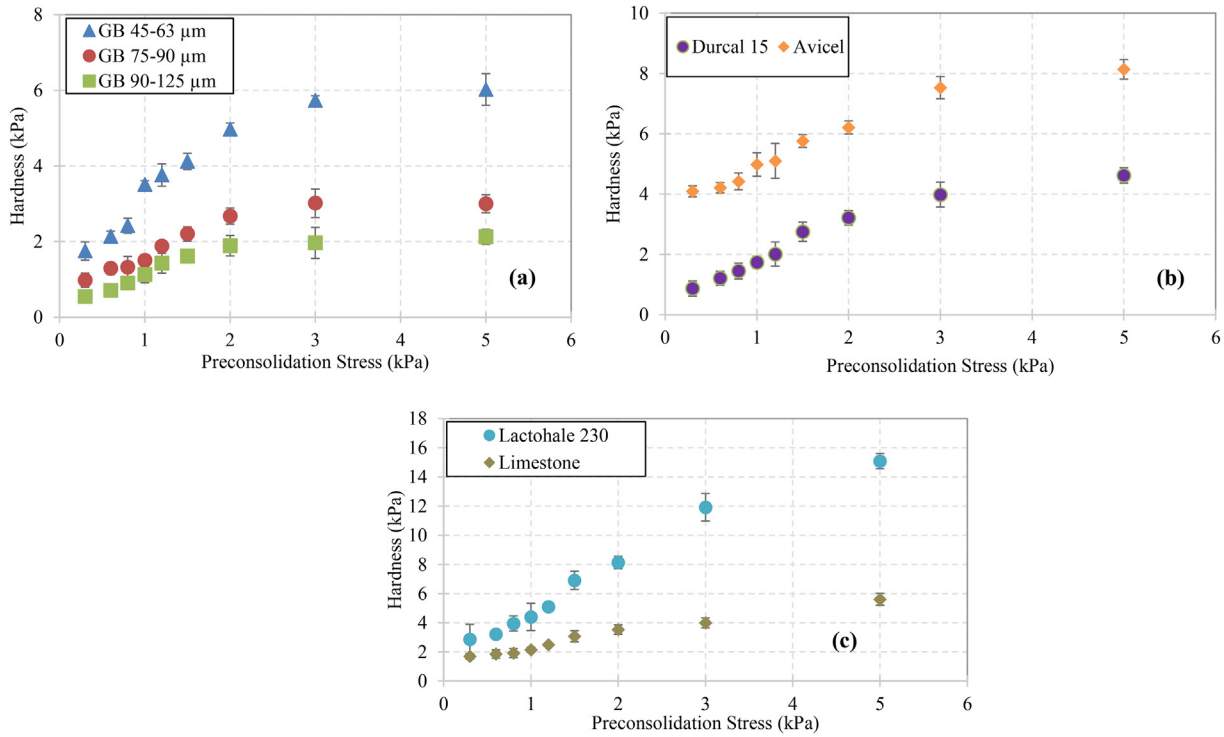
Fig. 8. Relationship between hardness and preconsolidation stress, including the at low stress levels for all the tested materials; (a): different sieve cuts of silanised glass beads; (b): Avicel and Durcal 15; (c): limestone and lactohale 230.
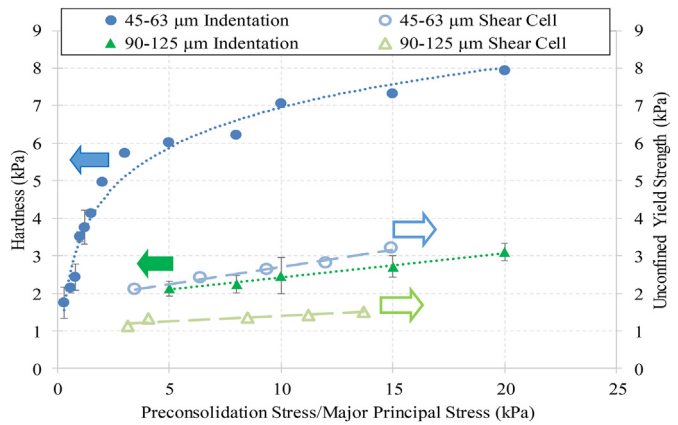

Fig. 9. Relationship between hardness measured by BIM and unconfined yield strength measured by the shear cell as a function of preconsolidation stress/major principal stress for two sieve cuts (45–63 μm and 90–125 μm) of silanised glass beads.
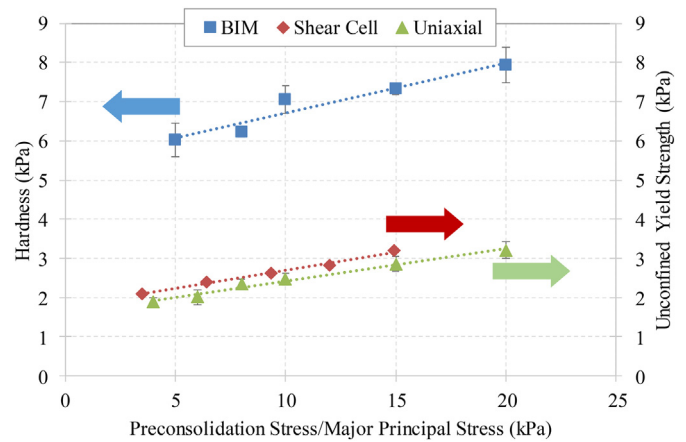

Fig. 10. Trends of hardness measured by BIM and unconfined yield strength measured by the shear cell and uniaxial compression for 45–63 μm silanised glass beads.

230 sample has the greatest hardness for a given preconsolidation stress, whilst 90–125 μm silanised glass beads have the lowest hardness value amongst all the tested materials.

4. Discussion

The unconfined yield strength and hardness, measured by the shear cell method and ball indentation, method respectively, for 45–63 μm and 90–125 μm silanised glass beads are shown together in Fig. 9. Here the hardness is plotted against the preconsolidation stress, whilst the unconfined yield strength is a function of the major principal stress so the abscissa has two representations for the same numerical figures. However, since the bed is vertically consolidated prior to indentation, and the indenter is driven vertically downward into the sample, the

preconsolidation stress does not differ greatly from the major principal stress. There is clearly a correlation between the unconfined yield strength (Y) and hardness (H) for both samples of silanised glass beads in the preconsolidation stress/major principal stress range of 3–20 kPa. The difference between these measurements obtained from the two techniques is due to the constraint factor (C) being greater than unity. The annular shear cell cannot be used reliably to carry out measurements at low applied stresses for these samples. In contrast the hardness can be measured at low preconsolidation stresses by indentation, as showing in Fig. 9 for 43–63 μm silanised glass beads. It is a common practice to extrapolate the flow function plot from shear cell measurements to low preconsolidation stresses to determine the flow function coefficient and bulk flow behaviour at very low stress levels (e.g. for powder flow from small containers and reservoirs). As shown in Fig. 9, this would lead to an underestimation of flow function
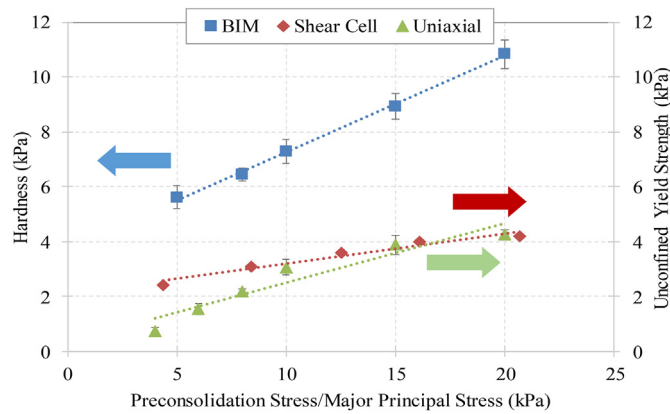
Fig. 11. Trends of hardness measured by BIM and unconfined yield strength measured by the shear cell and uniaxial compression for limestone powder sample.

coefficient below about 3 kPa. Therefore, an advantage of the ball indentation technique over other flow assessment methods is its ability to take measurement at stresses as low as 200 Pa.

The results of BIM, shear cell and uniaxial compression tests for 45–63 μm silanised glass beads are assembled in Fig. 10. The trend is linear for all the three cases and the unconfined yield strength obtained from the uniaxial compression and the shear cell tests are remarkably close. The slight variations are expected due to differences in the testing methods, giving rise to different stress histories and particle packing [38]. Also, in the ring shear tester there is no limit on the maximum shear strain, thus making it possible to always attain a critical state of deformation [39], whilst in the uniaxial compression test the internal deformation of the sample does not always ensure that the critical state is attained, which leads to lower values of the unconfined yield strength under the same major principal stress [7]. Nevertheless, a good agreement is observed between the uniaxial compression test and the shear cell in the case of silanised glass beads.

A similar comparison is shown in Fig. 11 for limestone. Here the uniaxial compression test gives a steeper slope as compared to the ring shear cell tester. This might be due to a change in the powder structure, reorientation and particle attrition in the shear plane. This has been shown to occur for some weak powder samples when a large shear stress is applied in the ring shear cell [13].

The uniaxial compression test and annular and translational shear tests have been compared for different materials by [13,38]. Good correlations have been reported between the two techniques for free flowing materials. However, for cohesive powders notable differences between the unconfined yield strength measured by uniaxial compression and shear cells tests have been reported by [6,10]; Maltby and Enstad, 1993. Such differences have been attributed to wall friction exerted on the powder sample during uniaxial compression. In the tests carried out have the wall material is PTFE and has a low friction, thus the two methods do not show major disparities.

4.1. Constraint factor

It is important to be able to infer the unconfined yield strength from the ball indentation measurement in order to provide a common base with the shear cell testing to assess powder flow. This requires characterisation of the constraint factor for each material. For this purpose, the unconfined yield strength as measured by the uniaxial compression test is used, as it gives a similar preconsolidation state to that used for indentation. This is shown in Fig. 12 for preconsolidation stresses in the range 5–20 kPa for all the test materials. The constraint factor is remarkably invariant with preconsolidation stress for Avicel, Durcal 15 and 75–90 μm silanised glass beads. There is a slight decrease in its value at high preconsolidation stresses for the other test materials within the range of preconsolidation stresses tested. Also, it decreases as the particle size is increased for the glass beads. The results clearly show that it varies significantly for different materials. Its value is low for glass beads and limestone and varies in the range 2–3, implying the flow due to indentation is least constrained for these materials. In contrast, its value is the largest for Lactohale 230 (6.5–7.8), presumably
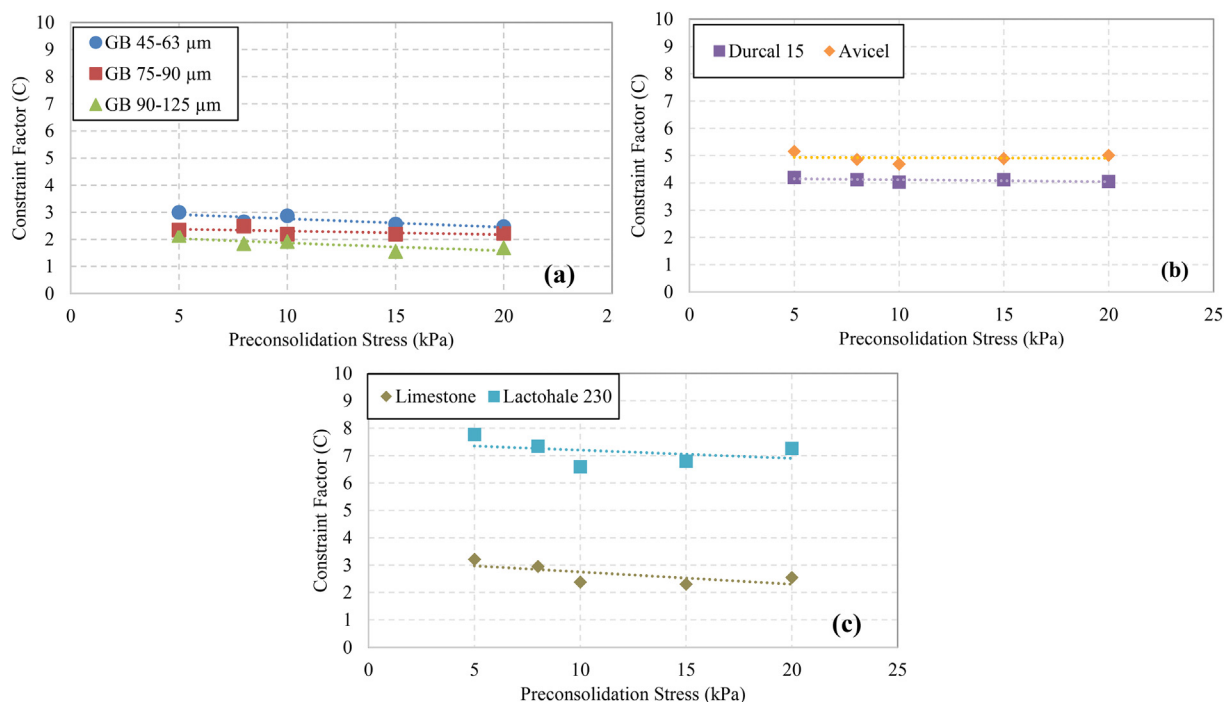

Fig. 12. Constraint factor variations with preconsolidation stress for all the materials tested (a): sieve cuts of silanised glass beads; (b): Avicel and Durcal 15; (c): limestone and Lactohale 230.

due to its particle shape and rugged surfaces causing particle interlocking and high friction. This is also to some extent the case for Avicel. However, it is very difficult to evaluate experimentally which properties influence the constraint factor most as there are many parameters which could be influential. Therefore, the most appropriate approach to analyse the dependency of *C* on particle properties is by numerical simulation by Discrete Element Method (DEM), where the influence of particle shape, size and its distribution, adhesion and friction can be analysed systematically by varying one parameter at a time. This has in fact been done for some of the parameters by Pasha et al. [30], but others such as particle shape and its combination with adhesion need to be addressed in future.

5. Conclusions

The flow resistance of bulk cohesive powders, as represented by hardness, has been evaluated by the ball indentation method. The method is particularly attractive for low applied stresses, as most other test methods cannot provide quantitative measurements in this range. Moreover it is the only viable method when a limited powder quantity is available. The conventional techniques, i.e. shear cell and uniaxial compression testers, use linear extrapolation for assessing powder behaviour at low stress levels. However, the change of the trend of hardness at low preconsolidation stresses implies that the linear extrapolation of either the bulk powder cohesion or unconfined yield strength values to low stresses from measurements made at higher stresses might not be reliable.

The unconfined yield strength as measured by the uniaxial compression and ring shear cell tester, shows a close agreement in the case of silanised glass beads as the die wall friction is small for this material. For limestone the two test methods give differing results at low stress levels, presumably due to the combined effect of wall friction and stress history. The constraint factor was determined from the unconfined yield strength by the uniaxial compression test and the hardness measured as by the ball indentation method. It remains fairly constant for the range of preconsolidation stresses applied but differs markedly for the test materials, implying the necessity for its characterisation for each material. These differences are presumably due to particle size distribution, shape, adhesion and friction. Elucidating these influencing factors requires a systematic study by numerical simulations, where each parameter can be changed, whilst keeping the others unchanged.

Declaration of Competing Interest

The authors declare that they have no known competing financial interests or personal relationships that could have appeared to influence the work reported in this paper.

Acknowledgement

References

[1] D. Geldart, E.C. Abdullah, A. Verlinden, Characterisation of dry powders, Powder Technol. 190 (1–2) (2009) 70–74.
[2] R.L. Carr, Evaluating flow properties of solids, Chem. Eng. 72 (3) (1965) 163–168.
[3] J. Schwedes, Review on testers for measuring flow properties, Granul. Matter 5 (1) (2003) 1–43.
[4] B.H. Kaye, J. Gratton-Liimatainen, N. Faddis, Part. Part. Syst. Charact. 12 (1995) 232–245.
[5] M. Patil, V. Kale, C. Tapre, Design and valication of Flowmex: an instrument for powder flow measurment, Int. J. Food Agricult. Vet. Sci. 2 (1) (2012) 40–46.
[6] D. Schulze, Discussion of Testers and Test Procedures. Powders and Bulk Solids, Springer Berlin Heidelberg, 2008 163–198.

[7] T.A. Bell, E.J. Catalano, Z. Zhong, J.Y. Ooi, J.M. Rotter, Evaluation of Edinburgh powder tester, International Congress on Particle Technology Nuremburg, Germany 2007, pp. 1–6.
[8] G. Calvert, N. Curcic, C. Redhead, H. Ahmadian, C. Owen, D. Beckett, M. Ghadiri, A new environmental bulk powder caking tester, Powder Technol. 249 (2013) 323–329.
[9] A. Jenike, Storage and Flow of Solids (Bull. No. 123), 1964 Salt Lake City.
[10] P.A. Kulkarni, R.J. Berry, M.S. Bradley, Review of the flowability measuring techniques for powder metallurgy industry, Proc. Inst. Mech. Eng. Part E: J. Process Mech. Eng. 224 (3) (2010) 159–168.
[11] D.M. Ashton, R. Farley, F.H.H. Valentin, An improved apparatus for measuring the tensile strength of powders, J. Scientific Instrum. 41 (12) (1964) 763–765.
[12] A. Vasilenko, S. Koynov, B.J. Glasser, F.J. Muzzio, Role of preconsolidation state in the measurement of bulk density and cohesion, Powder Technol. 239 (2013) 366–373.
[13] L. Parrella, D. Barletta, R. Boerefijn, M. Poletto, Comparison between a uniaxial compaction tester and a shear tester for the characterization of powder flowability, Kona Powder Part. 26 (2008) 178–189.
[14] M. Valverde, A. Castellanos, A. Ramos, A.T. Pe, M.A. Morgan, P.K. Watson, An automated apparatus for measuring the tensile strength and compressibility of fine cohesive powders, Rev. Sci. Instrum. 71 (7) (2000) 2791–2795.
[15] R. Girimonte, P. Bernardo, A. Minnicelli, B. Formisani, Experimental characterization of the cohesive behaviour of fine powders by the raining bed test, Powder Technol. 325 (2018) 373–380.
[16] A. Hassanpour, M. Ghadiri, Characterisation of flowability of loosely compacted cohesive powders by indentation, Part. Part. Syst. Charact. 24 (2) (2007) 117–123.
[17] R. Freeman, Measuring the flow properties of consolidated, conditioned and aerated powders — a comparative study using a powder rheometer and a rotational shear cell, Powder Technol. 174 (2006) 25–33.
[18] C. Hare, U. Zafar, M. Ghadiri, T. Freeman, J. Clayton, M. Murtagh, Analysis of the dynamics of FT4 powder rheometer, Powder Technol. 285 (2015) 123–127.
[19] W. Nan, M. Ghadiri, Y. Wang, Analysis of powder rheometry of FT4: effect of air flow, Chem. Eng. Sci. 162 (2017) 141–151.
[20] H. Salehi, D. Sofia, D. Schütz, D. Barletta, M. Poletto, Experiments and simulation of torque in Anton Paar powder cell, Part. Sci. Technol. 36 (4) (2018) 501–512.
[21] U. Zafar, G. Calvert, C. Hare, M. Ghadiri, R. Girimonte, B. Formisani, M.A.S. Quintanilla, J.M. Valverde, Comparison of cohesive powder flowability measured by Schulze shear cell, raining bed method, Sevilla powder tester and new ball indentation method, Powder Technol. 286 (2015) 807–816.
[22] J.L. Bucaille, S. Stauss, E. Felder, J. Michler, Determination of plastic properties of metals by instrumented indentation using different sharp indenters, Acta Mater. 51 (2003) 1663–1678.
[23] Y.T. Cheng, C.M. Cheng, Scaling relationships in conical indentation of elastic-perfectly plastic solids, Int. J. Solids Struct. 36 (1999) 1231–1243.
[24] B.R. Donohue, A. Ambrus, S.R. Kalidindi, Critical evaluation of the indentation data analyses methods for the extraction of isotropic uniaxial mechanical properties using finite element models, Acta Mater. 60 (2012) 3943–3952.
[25] J.S. Field, M.V. Swain, Determining the mechanical properties of small volumes of material from submicrometer spherical indentations, J. Mater. Res. 10 (1995) 101–112.
[26] D. Tabor, Indentation hardness: fifty years on a personal view, Philos. Mag. 74 (1996) 1207–1215.
[27] R. Hill, E.H. Lee, S.J. Tupper, The theory of wedge indentation of ductile materials, Proc. R. Soc. A: Math. Phys. Eng. Sci. 188 (1013) (1947) 273–289.
[28] A. Fischer-Cripps, Elastic plastic behaviour in materials loaded with a spherical indenter, J. Mater. Sci. 32 (1997) 727–736.
[29] U. Zafar, C. Hare, A. Hassanpour, M. Ghadiri, Ball indentation on powder beds for assessing powder flowability: analysis of operation window, Powder Technol. 310 (2017) 300–306.
[30] M. Pasha, C. Hare, M. Hassanpour, M. Ghadiri, Analysis of ball indentation on cohesive powder beds using distinct element modelling, Powder Technol. 233 (2013) 80–90.
[31] M. Kuentz, P. Schirg, Powder flow in an automated uniaxial tester and an annular shear cell: a study of pharmaceutical excipients and analytical data comparison, Drug Dev. Ind. Pharm. 39 (9) (2013) 1476–1483.
[32] G. Tan, D.A. Morton, I. Larson, On the methods to measure powder flow, Curr. Pharm. Des. 21 (40) (2015) 5751–5765.
[33] G.V. Barbosa-ca, Compression and compaction characteristics, Nutr. Res. 49 (2005).
[34] M.A.S. Quintanilla, The Sevilla powder tester: a tool for characterizing the physical properties of fine cohesive powders at very small consolidations, Kona Powder Part. 22 (2004) 66–81.
[35] K.G. Pitt, Tablet formulation, in: D.G. Tovey (Ed.), Pharmaceutical Formulation: The Science and Technology of Dosage Forms, 93-100, The Royal Society of Chemistry, London, 2018.
[36] J.C. Williams, A.H. Birks, D. Bhattacharya, The direct measurement of the failure function of a cohesive powder, Powder Technol. 4 (1971) 328–337.
[37] A.G. Stavrou, C. Hare, A. Hassanpour, C.-Y. Wu, Investigation of powder flowability at low stresses: influence of particle size and size distribution, Powder Technol. 364 (2020) 98–114.
[38] R. Freeman, J.R. Cooke, L.C.R. Schneider, Measuring shear properties and normal stresses generated within a rotational shear cell for consolidated and non-consolidated powders, Powder Technol. 190 (1–2) (2009) 65–69.
[39] Z. Zhong, J.Y. Ooi, J. Rotter, Nonlinear effects of blending on coal handling behaviour. Proceedings of the 'From powder to bulk', Institution of Mechanical Engineers Conference on Powder and Bulk Solid Handling 2000, pp. 17–26.
[40] K. Johanson, Personal Communication. Material Flow Equipment, LLC, 7010 NW23rd Way, Suite A, Gainesville, FL 32653 USA,, 2014 , http://www.matflowsol.com.